JOURNAL OF AEROSPACE COMPUTING, INFORMATION, AND COMMUNICATION
Vol. 8, January 2011

Cooperative Control of Multiple Uninhabited Aerial Vehicles for Monitoring and Fighting Wildfires

Manish Kumar*, Kelly Cohen*, and Baisravan HomChaudhuri*
University of Cincinnati, Cincinnati, Ohio 45221

DOI: 10.2514/1.48403

Uninhabited aerial vehicles provide numerous advantages in fighting wildland fires that include persistent operation and elimination of humans from performing what can be dull, dangerous, and dirty work. Multiple cooperating uninhabited aerial vehicles can potentially bring about a paradigm shift in the way we fight complex wildland fires. This paper investigates algorithmic development for cooperative control of a number of uninhabited aerial vehicles engaged in fighting a wildland fire. The paper considers two tasks to be performed by a group of uninhabited aerial vehicles: 1) Cooperative tracking of a fire front for accurate situational awareness, and 2) cooperative, autonomous fire fighting using fire suppressant fluid. The scenario considered in this paper makes the following assumptions: information regarding the location of the fire and position of all uninhabited aerial vehicles is made available to each uninhabited aerial vehicle; and each uninhabited aerial vehicle is equipped with unlimited fire suppressant fluid which extinguishes fire in a circle of specified area directly beneath it. This paper formulates these two tasks of fire fighting based upon optimization of respective utility functions, develops a decentralized control method for the cooperative uninhabited aerial vehicles, and analyzes the system for its stability and its ability to carry out the tasks. The proposed strategies have been verified with the help of extensive simulations. Although simplifying assumptions have been made, this preliminary study presents a framework for path planning and cooperative control of multiple uninhabited aerial vehicles engaged in gathering data and actively fighting forest fires.

Nomenclature

$f(.)$	effectiveness function for task 2
$h(q,t)$	shape function
N	number of UAVs
p_i	velocity of the ith UAV
$\mathbf{p}$	stacked velocity vector of all the UAVs
q	variable for representing position on the terrain
q_i	position of the ith UAV
$\mathbf{q}$	stacked position vector of all the UAVs
S	two-dimensional shape of fire
∂S	boundary of two-dimensional shape of fire
$U(\mathbf{q},t)$	utility function
$U^1(\mathbf{q},t)$	utility function for task 1
$U^2(\mathbf{q},t)$	utility function for task 2

Received 4 December 2009; accepted for publication 30 September 2010.
* School of Dynamic Systems, College of Engineering and Applied Science.

$V(\mathbf{q}, t)$	total potential of the system
$V^1(\mathbf{q}, t)$	total potential of the system for task 1
$V^2(\mathbf{q}, t)$	total potential of the system for task 2
V_{ij}	pair-wise potential between UAV i and j
$\dot{X}_T$	translational speed of the UAV
α	wind direction
θ	orientation of the UAV
$\phi(q, t)$	spatio-temporal distribution of fire
$\Psi(\mathbf{q}, \mathbf{p}, t)$	Lyapunov function
ω	rotational speed of the UAV

I. Introduction

IN RECENT years, in spite of large expenditures and substantial infrastructure dedicated to wildland fire fighting, the damage done in terms of acres burnt has risen dramatically and has reached record highs during the last couple of years. This is evident from the fact that, during 2005–2007, wildland fires have consumed approximately 27 million acres of land as per the data provided by National Interagency Fire Control [1]. The severity of the wildland fires can be judged from the fact that during a period of just two weeks, the October 2007 California wildland fires resulted in approximately 0.5 million acres of burnt land, evacuation of a million people, and had a price tag of over 1 billion dollars. Apart from these short-term socio-economic impacts, large wildland fires have smoke-related health impacts, and huge long-term environmental impacts. Mega wildland fires pump a large amount of carbon dioxide very quickly into the environment which can have a tremendous impact on climate. In a study carried out to estimate carbon dioxide (CO_2) emissions using computer models [2] for the October 2007 California fires, it was found that the fires produced 7.9 metric tons of CO_2 in just one week, which was equivalent to 25% of monthly CO_2 emissions due to burning of fossil fuels in California. Conventional fire-fighting methods are clearly inadequate in dealing with the mega wildland fires, and there is a need for a paradigm shift in the combating methodology. Uninhabited aerial vehicles (UAVs), working together with manned fixed wing and rotary wing aircraft, offer the possibility of realizing new and affordable technology which can make a difference in forest fire surveillance, monitoring, and control. Uninhabited aerial vehicles offer several advantages: they can be flown in dangerous situations; they can fly for longer duration enabling long-term data gathering and situational awareness; they can fly safely in bad weather conditions at higher altitudes; and they can be equipped with sensors such as daylight CCD cameras during day time and/or infra-red (IR) imaging during night time, and active fire-suppressants for semiautonomous operations. The UAVs can conduct surveillance on preprogrammed flight paths looking for fires, and upon hot spot or fire detection, they can provide the location and monitor the status. During fire-fighting operations, manned aircraft/UAV in conjunction with ground-based resources can be used to suppress/control the fire, and provide evacuation routes for people and equipment. Although satellites such as NASAs EO-1 and UAVs such as the Global Hawk and the Predator/Ikhana have been used in the recent fires, a highly probable future scenario would incorporate a hierarchy of several networked heterogeneous manned/unmanned aircrafts and ground-based assets cooperating intelligently.

This paper explores a *simplified scenario* in which wildland fire is fought with the help of autonomous UAVs. Two tasks are considered in this paper: 1) The UAVs, equipped with visual/IR sensors, are used to cooperatively track the fire-front perimeter to provide situational awareness; and 2) the UAVs, equipped with fire suppressant fluid, cooperatively extinguish fire. For both tasks, the UAVs can communicate with each other and provide their locations to the other UAVs. The location of the fire is made available to each UAV, and the objective of the system of multiple UAVs is to use the available information to 1) track the fire front or fire-boundary by persistently covering the fire front under the UAV footprints, and 2) suppress the fire in a cooperative manner. This paper formulates cooperative control strategies of multiple UAVs engaged in the two tasks.

During the past few years, a good deal of research has been carried out in the field of control and coordination of multiple mobile robots [3–20]. Advances in communication, increased computational capacity, miniaturization techniques, and novel control strategies have facilitated the use of a large number of autonomous mobile robots in a

cooperative manner which can find applications in a number of fields. Typical examples include planetary exploration, cooperative transport systems, distributed manufacturing systems, search and rescue operations, surveillance and reconnaissance operation, massive sensing operation using mobile ground or air vehicles, combat mission using a group of unmanned air vehicles, and land mine detection and disposal. In all such applications, the control, coordination, and management of a large number of robots operating in dynamic and uncertain conditions are the common underlying challenges. Researchers have been attempting to find correspondence of this problem in mathematical biology, statistical physics, computer graphics, and study of self-organizing behavior in nature such as those of birds and fish in order to draw inspirations that can be used to develop distributed control strategies for a group of mobile robots.

One of the very first applications of artificial formation was behavioral simulation of flocks of birds, herds of animals, and schools of fish for computer graphics by Reynolds [3]. He stated three simple behaviors that lead to flocking in birds and fish: collision avoidance, velocity matching, and flock centering (in decreasing order of precedence). Inspired by biological models of ant colonies/fish schools/herds, Reynolds' approach, and control-theoretic approaches, several techniques have been reported in the literature for control and coordination of multiple mobile robots. These approaches can be broadly classified into the following categories: behavior-based control, virtual structure or potential function-based approach, and leader–follower approach.

In behavior-based control [4,5], every agent or robot has a defined set of behaviors. The final control action is achieved by assigning appropriate weights to each of them. The group behavior emerges as a combination of group members' behaviors such as obstacle avoidance, collision avoidance, maintaining formation, and finding target. The problem is, then, to develop techniques to assign weights to different behaviors in order to achieve the desired group behavior. In the virtual structure approach, the entire formation is treated as a single structure. The desired motion is assigned to the virtual structure [6,7], which then derives the desired motion of individual robots. A few researchers [8–13] have used artificial potential functions to represent the interactions between robots. Ganguli et al. [14] and Martinez et al. [15] have developed innovative composite objective functions for various tasks such as area-coverage deployment, source detection, and boundary estimation. In a manner similar to artificial potential function-based methods, motion coordination is achieved via optimization of such objective functions. In the leader–follower approach, some robots are designated as leaders and others as followers. In this technique, a follower robot maintains a prespecified distance and orientation with respect to its leader or leaders. In this case, the stability of the system depends on the stability of individuals. Lately, there have been a number of studies using this approach such as in spacecraft formation control [16], mobile robot formation control [17], aircraft formation control, and cooperative robot control [18].

Application of multiple autonomous robots carrying out a mission in a cooperative manner is an area of extensive current study, and researchers have been trying to develop task-based controllers for coordination. The task of wildland fire fighting with the help of multiple UAVs is even more challenging due to the dynamic nature of fire growth and propagation which depends on several environmental factors and weather conditions. Closely related applications of multiple robots studied in the literature include coverage control [19] for large area sensing tasks and cooperative shape/pattern generation [20]. For example, the motion coordination problem for swarms of sensing agents has been investigated to maximize the information provided by these distributed agents, and has been treated within the framework of locational optimization problems. Similarly, shape generation algorithms have been developed to generate arbitrary shapes and patterns using swarms of robots. However, most of these problems have been studied for static cases, where the targets or the properties of the environment to be observed were stationary. The dynamic nature of forest fire propagation makes it particularly challenging to continuously and exhaustively keep the area under the fire in the footprint (area under the UAV which is within sensing/actuation zone) of UAVs. A lot of research has been carried out to understand the mechanism of forest fires growth, and accurate models to predict their propagation have been developed. These models can be used to predict the growth of forest fires, and accordingly coordinate the motion of UAVs. This paper formulates the problem of motion coordination and path planning of multiple UAVs working together to track the fire front and extinguish forest fire as an optimization of a utility function, and uses different simplified scenarios and a fire growth model based upon Huygen's principle [21] available in the literature to derive and verify results. The paper is organized as follows: first, the problems for the two tasks considered in this paper are formulated in terms of optimization of comprehensive utility functions. Then, a brief discussion on models for wildland fire growth available in the literature and the one used in this paper is presented. The distributed control

laws are then presented, accompanied by considerations in UAV formation constraint and analysis of the system under the distributed control law. Finally, extensive simulations are carried out to demonstrate the effectiveness of the proposed control strategies, followed by discussions and conclusions.

II. Problem Formulation

In this section, we present the problem formulation of the two fire-fighting tasks with the help of multiple UAVs by developing utility functions for respective tasks. A utility function represents a quantity whose minimization (or maximization) results in attaining the desired collective objective. We consider a two-dimensional terrain Q where any point is represented by $q \in Q \in R^m$, $m = 2$. The number of UAVs is N.

1) *Task 1*: *Cooperative tracking of fire front for accurate situational awareness:* Here, we assume the fire to be represented by a two-dimensional shape S, and the fire front (boundary of the forest fire) to be represented by the boundary ∂S of that shape. The fire front can be represented by a shape function $h : R^m \rightarrow R$ such that h is positive semidefinite in Q. For $q \in \partial S$, i.e., the points on the boundary of shape S, $h(q, t) = 0$. The objective of the multi-UAV team is to form a shape or pattern such that its distance to the fire-boundary is minimized (so that the UAV footprints cover the fire front) as well as the UAVs are distributed uniformly over the boundary. The utility function can be given by

$$U^1(\mathbf{q}, t) = \sum_{i=1}^{N} h(q_i, t) \tag{1}$$

where $q_i \in R^m$ is the position of the UAV i and $\mathbf{q} \in R^{mN}$ is the stacked position vector of all the UAVs. The utility function $U^1(\mathbf{q}, t) : R^{mN} \rightarrow R_{\geqslant 0}$ is a positive semidefinite quantity. This utility function provides a measure of proximity of the UAVs to the boundary ∂S.

2) *Task 2*: *Cooperative, autonomous fire fighting using fire suppressant fluid:* Let the spatial distribution of fire be represented by $\phi(q, t)$. Further, let us assume that the effectiveness of a UAV i, located at q_i, in suppressing fire at q is represented by a function $f(\|q - q_i\|)$, where $\|.\|$ represents a Euclidean norm (or distance). Assuming that effectiveness of the UAV in suppressing fire is maximum when the UAV is directly above the fire, such a function would be minimum when the distance $\|q - q_i\|$ is zero, and would be a monotonically increasing function of the distance. Then the utility function can be given by

$$U^2(\mathbf{q}, t) = \int_Q \sum_{i=1}^{N} f(\|q - q_i\|)\phi(q, t)\mathrm{d}q \tag{2}$$

The utility function $U^2(\mathbf{q}, t) : R^{mN} \rightarrow R_{\geqslant 0}$ is a positive semidefinite quantity. If a discrete or grid-based model for representing a forest fire is used, Eq. (2) can be represented by

$$U^2(\mathbf{q}, t) = \sum\nolimits_Q \sum_{i=1}^{N} f(\|q - q_i\|)\phi(q, t) \tag{3}$$

where

$$\begin{aligned} \phi(q, t) &= 1 \qquad \text{if cell at } q \text{ is on fire} \\ &= 0 \qquad \text{otherwise} \end{aligned}$$

The objective of the controls at any given time would be to minimize the utility function given by Eq. (2) for the continuous case, or Eq. (3) for the case where environment is modeled in a grid-based framework.

III. Fire Growth Models

To develop effective cooperative control strategies for forest fire fighting, it is imperative to model fire growth, represented by the function $\phi(q, t)$, from a spatio-temporal perspective. Integrating the many aspects of fire behavior (wind, terrain, temperature, humidity, fuel, etc.) is a very challenging task, and a lot of research has been carried

out over the last few decades. There are a couple of basic approaches to fire growth models, namely cellular and the two-dimensional deterministic wave approaches.

The cellular or the grid-based approach for fire growth is simulated in a discrete fashion on a regularly structured grid. A well-cited example of this modeling methodology was developed by Kourtz and O'Regan [22], which was based on a Monte Carlo technique. The model enables simulation of a small fire at any time after ignition by predicting the perimeter location and burning area for prescribed fuel and weather conditions. Although cellular models are simple and provide necessary insight for conceptual system studies, they need additional mechanisms to incorporate temporal changes such as shifting wind speed and direction as well as fuel moisture. For example, Karafyllidis and Thanailakis [23] have developed a model to predict fire growth using cellular automata that can predict fire growth accurately in homogeneous as well as heterogeneous conditions, and can easily incorporate weather conditions and land topography.

Some of the problems associated with cellular models are avoided by the vector or wave approach based on Huygen's principle [21] for fire growth modeling. This model has been used in this paper for fire propagation to test and validate the proposed cooperative motion control algorithms. This approach is incorporated into the fire growth model *FARSITE* (Fire Area Simulator [24]). FARSITE model is widely used by the USDI National Park Service, USDA Forest Service, and other federal and state land management agencies to simulate the spread of wildfires, and it automatically computes wildfire growth and behavior for long time periods under heterogeneous conditions of terrain, fuels, and weather. In this modeling technique, also called the envelop model, each point on the fire front is considered to be a new source of fire generation and the fire front is propagated as a continuously expanding fire polygon or ellipse at specified time-steps. The fire polygon is defined by a series of two-dimensional vertices (points with X, Y coordinates). The number of vertices increases as the fire grows over time (polygon expands [21]). The expansion of the fire polygon is determined by computing the spread rate and direction from each vertex and multiplying by the duration of the time-step. Assuming a uniform fuel distribution, uniform landscape and weather, and constant wind direction, fire fronts propagate in an elliptical fashion. Equations governing the Envelop Model are provided subsequently:

$$
\begin{aligned}
X_t &= \frac{a^2 \cos\alpha (x_s \sin\alpha + y_s \cos\alpha) - b^2 \sin\alpha (x \cos\alpha - y_s \sin\alpha)}{\sqrt{b^2 (x_s \cos\alpha + y_s \sin\alpha)^2 - a^2 (x_s \sin\alpha - y_s \cos\alpha)^2}} + c \sin\alpha \\
Y_t &= \frac{-a^2 \sin\alpha (x_s \sin\alpha + y_s \cos\alpha) - b^2 \cos\alpha (x \cos\alpha - y_s \sin\alpha)}{\sqrt{b^2 (x_s \cos\alpha + y_s \sin\alpha)^2 - a^2 (x_s \sin\alpha - y_s \cos\alpha)^2}} + c \cos\alpha
\end{aligned}
\tag{4}
$$

Here "X_t" and "Y_t" are the rate differentials and the angle α is the wind direction; and "x_s" and "y_s" are the orientation of the vertex on the fire front in the terms of component differentials. The location of the new fire front is available by multiplying the rate differentials with the step time. Figure 1a shows the propagation for uniform or

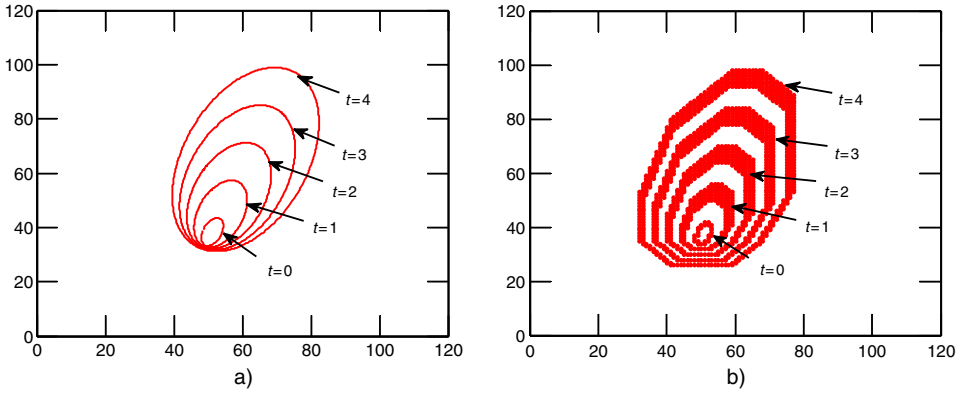

Fig. 1 Fire fronts obtained using the envelop model in homogeneous conditions at different time instants a) for a continuous case, and b) in a discrete grid-based framework.

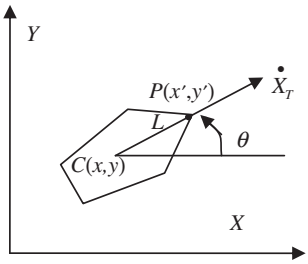

Fig. 2 Schematic representation of a mobile agent.

homogeneous fuel, topography, and weather conditions when the wind is flowing at an angle of 20° with Y-axis. Very often, these fire propagation models are overlaid on geographic information systems that provide other topographical information about the landscape and maps using multidimensional grids. Hence, it may be desirable to develop the Envelop model in a grid-based framework, which can be easily done by considering each point on the grid as a point on the fire front. The other mathematical formulations remain the same. For example, the fire propagation in Fig. 1a carried out in a continuous manner can also be carried out on a grid as shown in Fig. 1b. It should be noted that the grid-based model will not be exactly the same as the continuous model because of some discretization error.

IV. Distributed Control Law

The motion of a UAV is represented using the following kinematic unicycle model:

$$\begin{aligned} \dot{x} &= \dot{X}_T \cos\theta \\ \dot{y} &= \dot{X}_T \sin\theta \\ \dot{\theta} &= \omega \end{aligned} \tag{5}$$

where x and y represent the position of the UAV, $q = [x, y]^T$, θ represents the orientation, $\dot{X}_T$ is the translational speed, and ω is the rotational speed. A schematic diagram of the UAV model is represented in Fig. 2.

The kinematic model described earlier can be used to obtain the dynamic model of UAV control by considering the motion of point $P(x', y')$ on the UAV at distance L from the center $C(x, y)$. Let us assume that the UAV has a mass M and moment of inertia J. Differentiating Eqs. (5) gives

$$\begin{aligned} \ddot{x} &= \ddot{X}_T \cos\theta - \dot{\theta}\,\dot{X}_T \sin\theta \\ \ddot{y} &= \ddot{X}_T \sin\theta + \dot{\theta}\,\dot{X}_T \cos\theta \\ \ddot{\theta} &= \dot{\omega} \end{aligned} \tag{6}$$

Coordinates of point P can be expressed in terms of the UAVs orientation and coordinates of the center of gravity C.

$$\begin{bmatrix} x' \\ y' \end{bmatrix} = \begin{bmatrix} x + L\cos\theta \\ y + L\sin\theta \end{bmatrix} \tag{7}$$

Differentiating Eq. (7) twice yields the acceleration of point P:

$$\begin{bmatrix} \ddot{x}' \\ \ddot{y}' \end{bmatrix} = \begin{bmatrix} \ddot{x} - L\cos\theta \cdot \dot{\theta}^2 - L\sin\theta \cdot \ddot{\theta} \\ \ddot{y} - L\sin\theta \cdot \dot{\theta}^2 + L\cos\theta \cdot \ddot{\theta} \end{bmatrix} = u = \begin{bmatrix} u_x \\ u_y \end{bmatrix} \tag{8}$$

Also,

$$M\ddot{X}_T = F$$
$$J\ddot{\theta} = T \tag{9}$$

where F is the force, and T is the torque applied to the UAV. From Eqs. (6), (8), and (9)

$$u = \begin{bmatrix} u_x \\ u_y \end{bmatrix} = \begin{bmatrix} \frac{1}{M}\cos\theta & -\frac{L}{J}\sin\theta \\ \frac{1}{M}\sin\theta & \frac{L}{J}\cos\theta \end{bmatrix} \begin{bmatrix} F \\ T \end{bmatrix} + \begin{bmatrix} -\dot{X}_T \sin\theta \cdot \dot{\theta} - L\cos\theta \cdot \dot{\theta}^2 \\ +\dot{X}_T \cos\theta \cdot \dot{\theta} - L\sin\theta \cdot \dot{\theta}^2 \end{bmatrix} \tag{10}$$

The control inputs F and T can be found as follows:

$$\begin{bmatrix} F \\ T \end{bmatrix} = \begin{bmatrix} \frac{1}{M}\cos\theta & -\frac{L}{J}\sin\theta \\ \frac{1}{M}\sin\theta & \frac{L}{J}\cos\theta \end{bmatrix}^{-1} \times \left\{ \begin{bmatrix} u_x \\ u_y \end{bmatrix} - \begin{bmatrix} -\dot{X}_T \sin\theta \cdot \dot{\theta} - L\cos\theta \cdot \dot{\theta}^2 \\ +\dot{X}_T \cos\theta \cdot \dot{\theta} - L\sin\theta \cdot \dot{\theta}^2 \end{bmatrix} \right\} \tag{11}$$

With regard to the model used, the following may be noted. This model assumes a planar motion of the UAVs ($m = 2$), and does not take into account any change in altitude of the UAVs. This assumption makes sense for the fire-fighting application since the UAVs are required to operate at a particular altitude. Also, this model does not consider UAV motion constraints such as constraints on the radius of turns, turn rate, and linear and rotational velocities. Some of these constraints can be overcome by assuming that the sensors mounted on the UAVs are actuated so that even if the UAVs cannot maintain the intended flight paths due to constraints, the sensors would adequately orient themselves to observe the desired space. The focus of this paper is on development of multi-UAV coordination algorithms for dynamic perimeter and hot-spot tracking. Works exist in the literature that use a similar kinematic model and take into account various saturation constraints [25].

The distributed control law for the ith UAV is given by

$$u_i(\mathbf{q}, t) = -\nabla_{q_i} U(\mathbf{q}, t) + g_i^v \tag{12}$$

where $u_i(\mathbf{q}, t)$ represents the control for the ith UAV (acceleration given by Eq. (10)), the first term on the right-hand side represents the gradient descent term based on the utility function, and the second term represents the damping force. The term ∇_{q_i} represents the gradient with respect to coordinates (position) of UAV i: q_i. The damping term g_i^v is given by

$$g_i^v = -cp_i \tag{13}$$

where c is a scalar gain, p_i represents the velocity of UAV i.

A. UAV Formation Constraints

Multiple UAVs working together and using the same air space need to obey certain distance and formation constraints for a number of reasons. For example, to avoid collision, they should not come close to each other. Similarly, to avoid broken communication links, they should not wander far away. Additionally, in case of cooperative tracking of fire fronts, the UAVs should be as close to the fire front as possible but as far from each other (to cover the complete fire front) as possible. The minimization of the utility function given by Eq. (1) ensures the proximity of the UAVs to the fire front but not their uniform coverage of the complete fire front. Similarly, the utility function given by Eqs. (2) and (3) facilitate the coverage of area under fire by the UAVs but does not avoid collision. One way of achieving the above desirable behavior in the multi-UAV system is to introduce artificial potential function-based terms in the control laws. We propose the following two artificial potential functions for the two tasks considered in this paper.

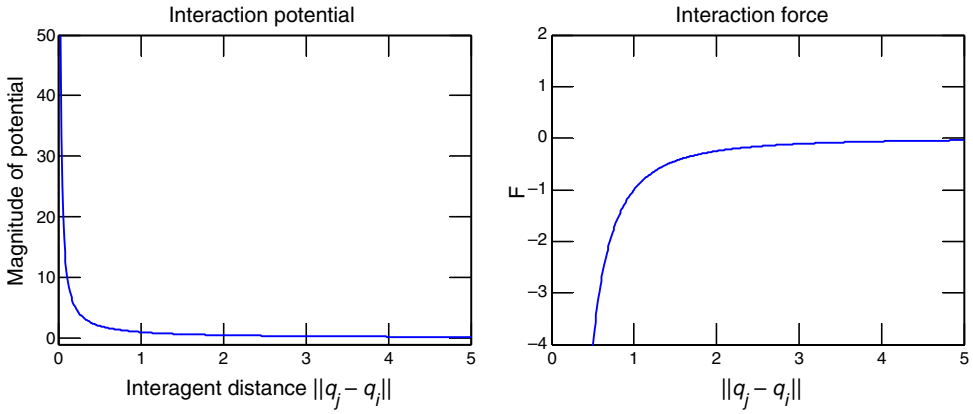

Fig. 3 Interaction potential (left) and the resulting force (right) as a function of inter-UAV distance.

Task 1: For task 1, we consider the following as a candidate [20] for artificial potential function resulting from interaction between two UAVs i and j:

$$V_{ij}^{1} = a\left(\frac{1}{\|q_j - q_i\|^{k}}\right) \tag{14}$$

where k is chosen so that the force resulting from the potential function becomes repulsive when two UAVs are physically near each other so that collision is avoided and the UAVs repel each other so that distance between them is maximized for better coverage of the fire front. When the UAVs are far from each other, the force is negligible. Figure 3 shows the potential and the force resulting from the potential plotted against the inter-UAV distance when $k = 1$. A negative value of the interaction force represents repulsion between two UAVs.

Task 2: For task 2, we propose the following artificial potential function [10–13] acting between two UAVs i and j with an attraction/repulsion profile:

$$V_{ij}^{2} = a\left(\ln(\|q_j - q_i\|) + \frac{d_0}{\|q_j - q_i\|}\right) \tag{15}$$

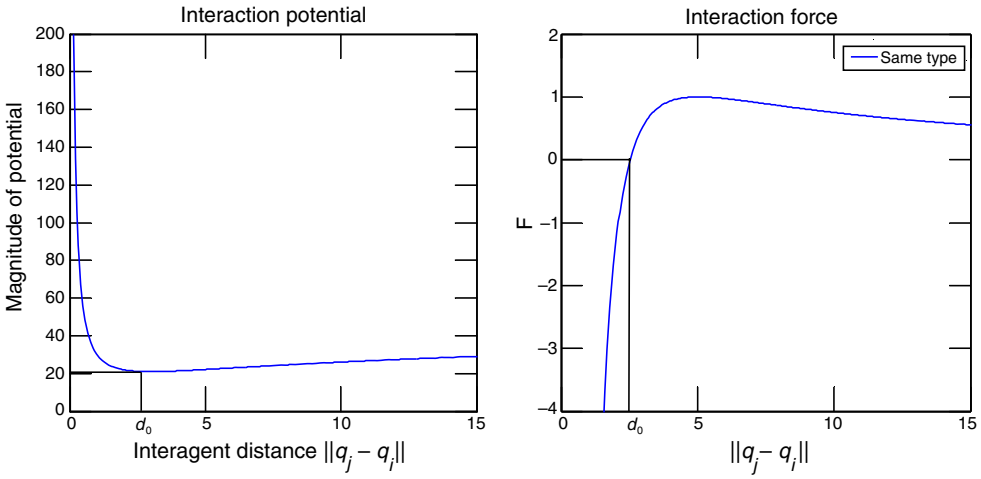

Fig. 4 Interaction potential (left) and the resulting force (right) as a function of inter-UAV distance.

Figure 4 shows the potential and the force resulting from the potential plotted against the inter-UAV distance. A positive value of force indicates an attractive force, and a negative value indicates repulsive force. As indicated in the figure, the potential becomes minimum (and force becomes zero) when the inter-agent distance is d_0.

B. Analysis of the Controller

Total potential $V(\mathbf{q}) : R^{mN} \rightarrow R_{\geqslant 0}$ of the system is given by

$$V(\mathbf{q}) = \frac{1}{2} \sum_{i=1}^{N} \sum_{\substack{j=1 \\ j \neq i}}^{N} V_{ij} \tag{16}$$

where V_{ij} is obtained from Eq. (14) for task 1 from and Eq. (15) for task 2. The distributed control law given by Eq. (12) can be modified to

$$u_i(\mathbf{q}, t) = -\nabla_{q_i} U(\mathbf{q}, t) - \nabla_{q_i} V(\mathbf{q}) + g_i^v \tag{17}$$

where $\nabla_{q_i} V(\mathbf{q})$ represents the gradient of the total potential $V(\mathbf{q})$ with respect to the position of UAV i.

The collective dynamics of the system is given by

$$\begin{aligned} \dot{\mathbf{q}} &= \mathbf{p} \\ \dot{\mathbf{p}} &= -\nabla V(\mathbf{q}) - \nabla U(\mathbf{q}, t) - c\mathbf{p} \end{aligned} \tag{18}$$

where $\mathbf{p} \in R^{mN}$ is the stacked velocity vector for all UAVs. To carry out stability analysis of the collective motion of agents resulting from this method, a Lyapunov function can be chosen as the sum of total energy (artificial potential energy and kinetic energy) and total utility of the system:

$$\Psi(\mathbf{q}, \mathbf{p}, t) = V(\mathbf{q}) + U(\mathbf{q}, t) + \frac{1}{2}\mathbf{p}^T\mathbf{p} \tag{19}$$

Proposition 1: Consider a system of N UAVs. Each of the UAVs follows dynamics given by Eqs. (5–12), and with a feedback control law given by Eq. (17). For any initial condition belonging to the level set of $\Psi(\mathbf{q}, \mathbf{p}, t)$ given by $\Omega_C = \{(\mathbf{q}, \mathbf{p}, t) : \Psi(\mathbf{q}, \mathbf{p}, t) \leqslant C\}$ with $C > 0$, and when the underlying graph of the system is complete, the uniform asymptotic stability of the system is guaranteed by an upper bound on the rate of growth of fire that depends on the velocities of the UAVs.

Proof: Differentiating $\Psi(\mathbf{q}, \mathbf{p}, t)$ with respect to time and using Eq. (18), one gets

$$\begin{aligned} \dot{\Psi}(\mathbf{q}, \mathbf{p}, t) &= \mathbf{p}^T \nabla V(\mathbf{q}) + \mathbf{p}^T \nabla U(\mathbf{q}, t) + \frac{\partial U(\mathbf{q}, t)}{\partial t} + \mathbf{p}^T \dot{\mathbf{p}} \\ &= \mathbf{p}^T \nabla V(\mathbf{q}) + \mathbf{p}^T \nabla U(\mathbf{q}, t) + \frac{\partial U(\mathbf{q}, t)}{\partial t} + \mathbf{p}^T(-\nabla V(\mathbf{q}) - \nabla U(\mathbf{q}, t) - c\mathbf{p}) \\ &= \frac{\partial U(\mathbf{q}, t)}{\partial t} - c\mathbf{p}^T\mathbf{p} \end{aligned} \tag{20}$$

From extension of Lasalle's Invariance Principle to nonautonomous systems [26,27], all solutions of the system starting in Ω_C will converge to the largest invariant in set $\Omega_I = \left\{(\mathbf{q}, \mathbf{p}) \in \Omega_I : \dot{\Psi}(\mathbf{q}, \mathbf{p}, t) = 0\right\}$, if $\dot{\Psi}(\mathbf{q}, \mathbf{p}, t) \leqslant 0$

$\forall t \geqslant 0$. This happens when

$$\frac{\partial U(\mathbf{q}, t)}{\partial t} \leqslant c\mathbf{p}^T\mathbf{p} \qquad \forall t \geqslant 0 \tag{21}$$

For task 1, Eq. (21) boils down to

$$\sum_{i=1}^{N} \frac{\partial h(q_i, t)}{\partial t} \leqslant c\mathbf{p}^T\mathbf{p} \qquad \forall t \geqslant 0 \tag{22}$$

And, for task 2, Eq. (21) boils down to

$$\int_Q \sum_{i=1}^{N} f\left(\|q - q_i\|\right) \frac{\partial \phi(q, t)}{\partial t} dq \leqslant c\mathbf{p}^T\mathbf{p} \qquad \forall t \geqslant 0 \tag{23}$$

Hence, Proposition 1 provides information on the bounds on the rate of growth of fire, $\partial h(q_i, t)/\partial t$ and $\partial \phi(q, t)/\partial t$, as a function of velocities of the UAVs. ■

Proposition 2: Consider a system of$N$ UAVs. Each of the UAVs follows dynamics given by Eqs. (5–12), and with a feedback control law given by Eq. (17). For any initial condition belonging to the level set of $\Psi(\mathbf{q}, \mathbf{p}, t)$, given by $\Omega_C = \{(\mathbf{q}, \mathbf{p}, t) : \Psi(\mathbf{q}, \mathbf{p}, t) \leqslant C\}$ with $C > 0$, $C < C^* = V(0)\left(V(0) = V_{ij}|_{\|q_j - q_i\|=0}\right)$, and the system satisfying conditions given by Eqs. (22) and (23) two UAVs will never collide for all $t \geqslant 0$.

Proof: This proposition can be proved by contradiction. Let us assume that at time $t = t_1 \geqslant 0$, two UAVs k and $l$collide, i.e., $q_k(t_1) = q_l(t_1)$. Hence, total potential of the system at time t_1, as given by Eq. (16) is obtained:

$$V(\mathbf{q}(t_1)) = \frac{1}{2}\sum_{i=1}^{N}\sum_{\substack{j=1 \\ j\neq i}}^{N} V_{ij} = V_{kl} + \frac{1}{2}\sum_{\substack{i=1 \\ i\neq k,l}}^{N}\sum_{\substack{j=1 \\ j\neq i,k,l}}^{N} V_{ij} = V(0) + \frac{1}{2}\sum_{\substack{i=1 \\ i\neq k,l}}^{N}\sum_{\substack{j=1 \\ j\neq i,k,l}}^{N} V_{ij} \geqslant V(0) =: C^* \tag{24}$$

Hence, $V(\mathbf{q}(t_1)) \geqslant C^*$. Also, from Eq. (19), and recalling that $U(\mathbf{q}, t_1)$ and $\mathbf{p}^T\mathbf{p}$ are positive semidefinite, we have

$$V(\mathbf{q}(t_1)) = \Psi(\mathbf{q}, \mathbf{p}, t_1) - U(\mathbf{q}, t_1) - \frac{1}{2}\mathbf{p}^T\mathbf{p} \leqslant \Psi(\mathbf{q}, \mathbf{p}, t_1) \leqslant C < C^* \tag{25}$$

which contradicts the earlier inequality $V(\mathbf{q}(t_1)) \geqslant C^*$. Therefore, by contradiction, no two UAVs will collide with each other. ■

V. Simulation Results and Discussion

The effectiveness of the proposed control strategy to cooperatively track fire fronts (task 1) and actively fight forest fires (task 2) with the help of multiple UAVs was verified via extensive simulations. For both the tasks, a two-dimensional environment is considered, and hence the position of a point in the terrain is given by $q = (x, y)$. The results obtained from simulations are provided below.

A. Task 1

A total number of 10 UAVs were used. The envelop model based upon Huygen's principle was used for simulating the fire. Homogeneous topography, vegetation, and weather conditions (including wind direction and velocity) were used. As we saw in Section III, under homogeneous conditions, the fire front takes the shape of an ellipse. Based upon the fire-front points generated by the simulated fire, the parameters of the elliptical shape function given by the following equation were obtained:

$$\frac{[\cos\alpha(x - x_c) + \sin\alpha(y - y_c)]^2}{e^2} + \frac{[-\sin\alpha(x - x_c) + \cos\alpha(y - y_c)]^2}{f^2} = 1 \tag{26}$$

where α is the angle made by the major axis of the ellipse with the Y-axis of the 2D world, $x, y \in q$, (x_c, y_c) is the center of the ellipse, and e and f are the lengths of semimajor and semiminor axes, respectively. Once the fire-front

points are obtained using the envelop model, the parameters of the ellipse, i.e., x_c, y_c, e, f, α are obtained. It may be noted that these parameters represent the dynamic fire front and hence are functions of time. The objective of the multi-UAV system is to track this elliptical boundary. The positive semidefinite shape function $h(q_i, t)$ used in Eq. (1) is obtained using

$$h(q_i, t) := \left\{ \frac{[\cos\alpha(x_i - x_c) + \sin\alpha(y_i - y_c)]^2}{e^2} + \frac{[-\sin\alpha(x_i - x_c) + \cos\alpha(y_i - y_c)]^2}{f^2} - 1 \right\}^2 \tag{27}$$

The distributed control law for each agent is obtained by Eq. (17) where $U(\mathbf{q}, t)$ is given by Eq. (1), and $V(\mathbf{q})$ is obtained using Eqs. (14) and (16) assuming $k = 1$. After substituting these values, the distributed control law is given by

$$\begin{aligned} u_i(\mathbf{q}, t) = &-\nabla_{q_i} \left(\left\{ \frac{[\cos\alpha(x_i - x_c) + \sin\alpha(y_i - y_c)]^2}{e^2} + \frac{[-\sin\alpha(x_i - x_c) + \cos\alpha(y_i - y_c)]^2}{f^2} - 1 \right\}^2 \right) \\ &- \sum_{\substack{j=1 \\ j \neq i}}^{N} a\left(\frac{(q_j - q_i)}{\|q_j - q_i\|^2} \right) - cp_i \end{aligned} \tag{28}$$

Figures 5 and 6 show the configurations of the UAVs forming an elliptical pattern under the application of the proposed control law. Figure 5 shows a case when the ellipse is stationary, i.e., it is not changing with time. Initially, the UAVs (shown by blue squares) are located randomly as shown in Fig. 5a. Upon application of the control law, the UAVs converge to the boundary of the ellipse as shown in Fig. 5b and c. For forest fire application, when the fire ellipse grows with time, the results are shown in Fig. 6. Figure 6a shows the initial conditions with an initial fire ellipse and random UAV configuration. Figure 6b–c shows that the UAVs track the elliptical fire front as it grows with time.

B. Task 2

A total number of 10 UAVs were used, and each UAV could suppress fire in a circular region of radius 10 m directly beneath it. Also $f(\|q - q_i\|)$ used in Eqs. (2) and (3) was assumed to be logarithmic:

$$f(\|q - q_i\|) = b\left(\ln(\|q - q_i\|) + \frac{d}{\|q - q_i\|} \right) \tag{29}$$

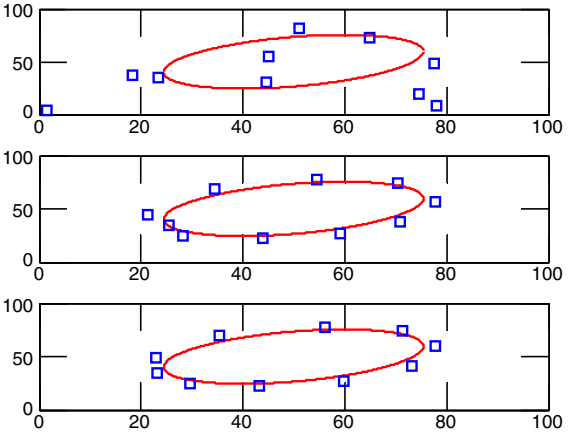

Fig. 5 Configuration of UAVs generating stationary ellipse pattern at different time instants (from top to bottom) a) $t = 0$ min (top), b) $t = 2.5$ min (middle), and c) $t = 5$ min (bottom).

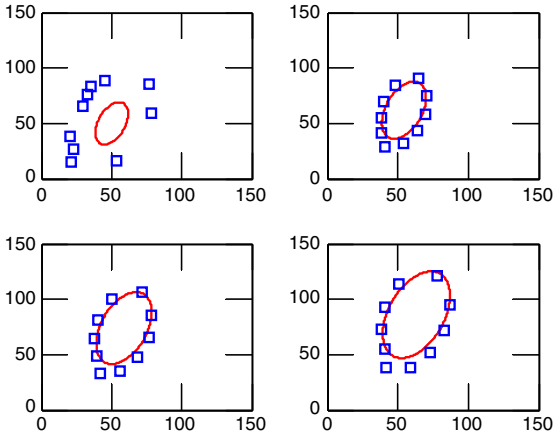

Fig. 6 The configuration of UAVs and fire fronts at different time instants (from left to right: a) $t = 0$ min, b) $t = 1.67$ min, c) $t = 3.33$ min, and d) $t = 5$ min).

where b is a parameter that provides a weight to the function, and d is a parameter that is chosen to be arbitrarily small. The distributed control law, as obtained from Eq. (17), becomes

$$u_i(\mathbf{q},t) = -\nabla_{q_i}\left\{\sum\nolimits_Q \sum_{i=1}^{N} b\left(\ln(\|q-q_i\|)+\frac{d}{\|q-q_i\|}\right)\phi(q,t)\right\}$$
$$-\nabla_{q_i}\left\{\sum_{i=1}^{N}\sum_{\substack{j=1\\ j\neq i}}^{N} a\left(\ln\left(\|q_j-q_i\|\right)+\frac{d_0}{\|q_j-q_i\|}\right)\right\} - cp_i \tag{30}$$

or

$$u_i(\mathbf{q},t) = -\left\{\sum\nolimits_Q b\left(\frac{1}{\|q-q_i\|}-\frac{d}{\|q-q_i\|^2}\right)\frac{(q-q_i)}{\|q-q_i\|}\phi\,(q,t)\right\}$$
$$-\left\{\sum_{\substack{j=1\\ j\neq i}}^{N} a\left(\frac{1}{\|q_j-q_i\|}-\frac{d_0}{\|q_j-q_i\|^2}\right)\frac{(q_j-q_i)}{\|q_j-q_i\|}\right\} - cp_i \tag{31}$$

Fire growth was modeled using the envelope model in a grid-based framework under homogeneous conditions. The whole terrain of area 100×100 m was divided into grid cells of size 1×1 m. Simulation results are provided for two distinct initial conditions: 1) single initial hot spot, and 2) two initial hot spots. These hot spots are created by initiating fires (at one location for the first case and at two locations for the second case). Once initiated, the fires are allowed to propagate for some time before actual suppression action by the UAVs begins.

1. Single Initial Hot Spot

The UAVs were randomly distributed initially over the terrain of size 100×100 m. Upon the initiation of their control at time $t = 0$ min, the UAVs start moving toward the current location of the fire in accordance with Eq. (31). Figure 7 shows the fire growth and UAVs positions at different instants of time. The UAV positions are shown by blue squares, currently burning cells are shown by red dots, and burnt cells are shown by black dots. Figure 8 shows a plot of a number of cells on fire plotted against time. The number of cells on fire becomes zero just before the 5 min time mark, indicating that the fire has been fully contained.

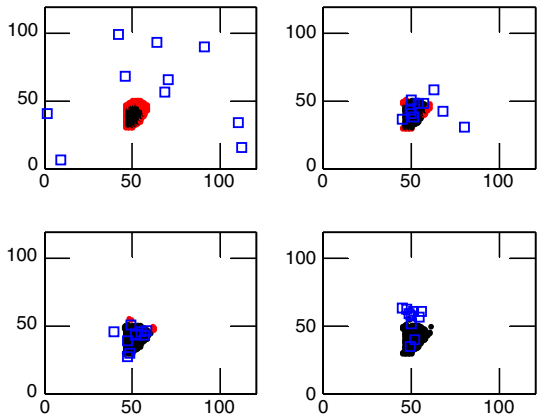

Fig. 7 The configuration of UAVs and state of fire at different time instants (from left to right: a) $t = 0$ min, b) $t = 1.67$ min, c) $t = 3.33$ min, and d) $t = 5$ min).

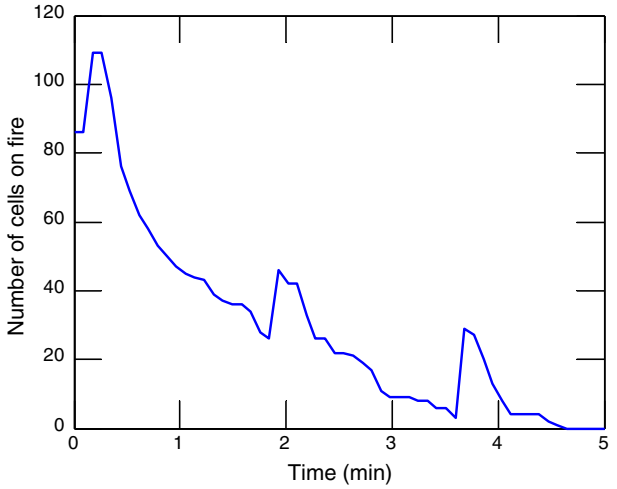

Fig. 8 Number of grid cells on fire vs. time for the case of single initial fire spot.

2. Multiple Initial Hot Spots

In this case, the fire was initiated at two cells (at position (25,25) and (75,75) as seen as dots in Fig. 9a). The UAVs were randomly distributed initially over the terrain of size 100×100 m. Figure 9 shows the growth of fire and positions of UAVs at different instants of time. Figure 10 shows the graph of a number of grids on fire plotted against time. It can be again seen that the UAVs were able to extinguish the fire in approximately 10 min.

One of the issues with the decentralized control law given by Eq. (17), which is based on gradient descent, is the issue of local minimum. This control law would lead the configuration of UAVs to a local minimum configuration (where the gradients of potential and utility functions are zero). It is not guaranteed that this configuration globally optimizes the designed utility function (so that fire fronts are optimally covered for task 1 and fire areas are optimally covered for task 2). However, the dynamic nature of the problem ensures that the local minimum changes, and that the UAVs are not stuck in those configurations for long. The scope of this preliminary paper is limited to developing strategies for path planning and cooperative control of multiple UAVs. There are several aspects of research that need to be carried out before such a system can be realized in practical wildfire fighting applications. For example, it may be noted that the assumption that each UAV has unlimited fire suppressant fluid is not practically implementable. In the real world, each UAV would have to return to its base after it has exhausted its fire suppressant fluid. A

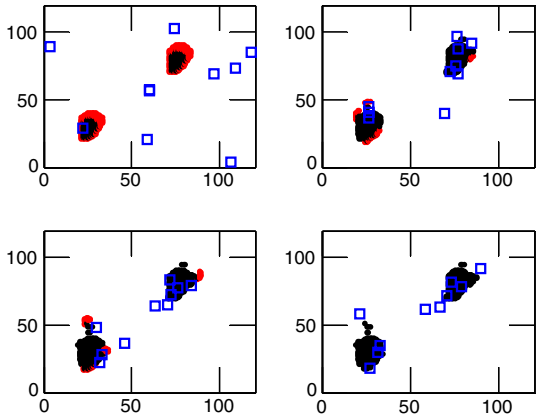

Fig. 9 The configuration of UAVs and state of fire at different time instants for the case of two initial fire spots (from left to right: a) $t = 0min$, b) $t = 3.33$ min, c) $t = 6.77$ min, and d) $t = 10$ min).

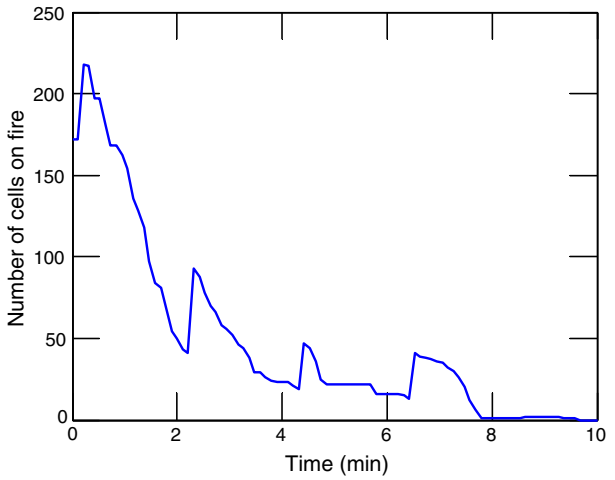

Fig. 10 Number of grid cells on fire vs. time for the case of two initial fire spots.

comprehensive strategy would consist of a hybrid hierarchical control scheme, where upper level control would allocate UAVs and determine the discrete state of the UAVs (e.g., engaged in active fire fighting, returning to base for refueling/loading fire suppressant, or engaged in fire monitoring). The methods developed in this paper would form the lower level control strategies for cooperative motion control of UAVs selected for a particular task. Similarly, the kinematic/dynamic model used in this paper does not consider UAV constraints and control saturation limits. A systematic study of cooperative control laws which incorporates these constraints will be an interesting future area of work. Also, two-dimensional motion considered in this paper has limitations where the terrain is three-dimensional (mountainous regions).

VI. Conclusion

This paper investigates the possibility of the use of UAVs in the monitoring, control, and mitigation of wildland fires. Multiple UAVs working together in a cooperative manner present a powerful and promising tool in monitoring, data gathering, generating situational awareness as well as in active fire fighting. This paper formulates the two tasks in forest fire fighting: monitoring and suppression, and presents those tasks as optimization problems. The paper provides a candidate utility function for each task. The distributed control law for coordinated motion control of multiple UAVs for each task is obtained using a gradient descent technique that optimizes the corresponding utility

functions as well as maintains flight constraints and avoids collisions. The system of UAVs under the distributed control laws for each task and their ability to cooperatively carry out the tasks are analyzed in a Lyapunov framework to obtain results on the bounds of the fire growth relating to velocities of UAVs as well as the numbers of them being used. Extensive simulation studies demonstrated the effectiveness of the proposed method in monitoring and suppressing forest fires. Future research would involve incorporating a more sophisticated benchmark problem with several simultaneous fire hot spots and heterogeneous fire conditions, and will involve areas with different priorities.

References

[1] National Fire News, National Interagency Fire Center, "Fire Information—Wildland Fire Statistics," [online database], http://www.nifc.gov/fire_info/fires_acres.htm [retrieved 21 July 2010].

[2] Wiedinmyer, C., and Neff, J. C., "Estimates of CO_2 from Fires in the United States: Implications for Carbon Management," *Carbon Balance Management*, Vol. 2, No. 10, 2007. doi:10.1186/1750-0680-2-10.

[3] Reynolds, C., "Flocks, Birds, and Schools: A Distributed Behavioral Model," *Computer Graphics*, Vol. 21, 1987, pp. 25–34.

[4] Balch, T., and Arkin, R., "Behavior-Based Formation Control for Multirobot Systems," *IEEE Transactions on Robotics and Automation,* Vol. 14, No. 6, 1998, pp. 926–939.

[5] Kube, C. R., and Zhang, H., "Collective Robotic Intelligence," *Proceedings of the Second International Conference on Simulation of Adaptive Behavior: From Animals to Animats*, MIT Press, Cambridge, MA, 1992, pp. 460–468.

[6] Ren, W., and Beard, R. W., "A Decentralized Scheme for Spacecraft Formation Flying via the Virtual Structure Approach," *Journal of Guidance, Control and Dynamics,* Vol. 27, No. 1, Jan.–Feb. 2004, pp. 73–82.

[7] Egerstedt, M., and Hu, X., "Formation Constrained Multi-agent Control," *Proceedings of the IEEE International Conference on Robotics and Automation,* Seoul, Korea, 2001, pp. 3961–3966.

[8] Olfati-Saber, R., "Flocking for Multi-agent Dynamic Systems: Algorithms and Theory," *IEEE Transactions on Automatic Control*, Vol. 51, No. 3, March 2006, pp. 401–420.

[9] Leonard, N., and Fiorelli, E., "Virtual Leaders, Artificial Potentials and Coordinated Control of Groups," *Proceedings of the IEEE Conference on Decision and Control*, Orlando, FL, 2001.

[10] Kumar, M., Milutinović, D., and Garg, D., "Role of Stochasticity in Self-organization of Robotic Swarms," *Proceedings of the American Control Conference*, Seattle, WA, 2008, pp. 123–128.

[11] Kumar, M., Garg, D., and Zachery, R., "Control of Multiple Mobile Agents based on Local Interactions via Artificial Potential Functions and Random Motion," *Proceedings of the ASME International Mechanical Engineering Congress and Exposition*, Chicago, IL, 2007, Paper No. IMECE2007-41521.

[12] Kumar, M., Garg, D., and Kumar, V., "Segregation of Heterogeneous Units in a Swarm of Robotic Agents," *IEEE Transactions on Automatic Control*, Vol. 55, No. 3, March 2010, pp. 743–748.

[13] Kumar, M., Garg, D., and Kumar, V., "Self-sorting in a Swarm of Heterogeneous Agents," *Proceedings of the American Control Conference*, Seattle, WA, 2008, pp. 117–122.

[14] Ganguli, A., Susca, S., Martinez, S., Bullo, F., and Cortes, J., "On Collective Motion in Sensor Networks: Sample Problems and Distributed Algorithms," *Proceedings of the IEEE Conference on Decision and Control*, Seville, Spain, Dec. 2005, pp. 4239–4244.

[15] Martinez, S., Bullo, F., Cortes, J., and Frazzoli, E., "On Synchronous Robotic Networks Part I: Models, Tasks, and Complexity Notions," *Proceedings of IEEE Conference on Decision and Control and European Control Conference*, Seville, Spain, Dec. 2005, pp. 2847–2852.

[16] Wang, P. K. C., and Hadaegh, F. Y., "Coordination and Control of Multiple Microspacecrafts Moving in Formation," *Journal of Astronautical Sciences*, Vol. 44, No. 3, 1996, pp. 315–355.

[17] Tanner, H. G., Pappas, G. J., and Kumar, V., "Leader-to-Formation Stability," *IEEE Transactions on Robotics and Automation,* Vol. 20, 2004, pp. 443–455.

[18] Sugar, T., and Kumar, V., "Decentralized Control of Cooperating Mobile Manipulators," *Proceedings of the IEEE International Conference on Robotics and Automation*, Leuven, Belgium, 16–21 May 1998, pp. 2916–2921.

[19] Cortes, J., Martinez, S., Karatas, T., and Bullo, F., "Coverage Control for Mobile Robot Sensing Networks," *Proceedings of the IEEE International Conference on Robotics & Automation*, Washington, DC, May 2002, pp. 1327–1332.

[20] Hsieh, M. A., Kumar, V., and Chainmowicz, L., "Decentralized Controllers for Shape Generation with Robotic Swarms," *Robotica*, Vol. 26, 2008, pp. 691–701.

[21] Richards, G. D., "An Elliptical Growth Model of Forest Fire Fronts and its Numerical Solution," *International Journal of Numerical Methods in Enginering*, Vol. 30, 1990, pp. 1163–1179.

[22] Kourtz, P., and O'Regan, W. G. "A Model for a Small Forest Fire…to Simulate Burned and Burning Areas for Use in a Detection Model," *Forest Science*, Vol. 17, No. 2, 1971, pp. 163–169.

[23] Karafyllidis, I., and Thanailakis, A., "A Model for Predicting Forest Fire Spreading Using Cellular Automata," *Ecological Modelling*, 1997, pp. 87–97.
[24] Finney, M. A, *"FARSITE*: Fire Area Simulator—Model Development and Evaluation," 2004, USDA Forest Service, Rocky Mountain Research Station, Research Paper RMRS-RP-4 Revised.
[25] Ren, W., and Beard, R. W., "CLF—Based Tracking Control for UAV Kinematic Models with Saturation Constraints," *Proceedings of the IEEE Conference on Decision and Control*, Maui, Hawaii, USA, 2003, pp. 3924–3929.
[26] Iggidr, A., and Sallet, G., "On the Stability of Nonautonomous Systems," *Automatica,* Vol. 39, 2003, pp. 167–171.
[27] Vidyasagar, M., *Nonlinear Systems Analysis*, SIAM, Philadelphia, PA, 2002.

Ella Atkins
Associate Editor